# A LOW TEMPERATURE GYROSCOPE CLOCK FOR GRAVITATIONAL REDSHIFT EXPERIMENTS

Saps Buchman, J. P. Turneaure, T. Walter, and C. W. Francis Everitt
*W. W. Hansen Experimental Physics Laboratory, Stanford University, Stanford, U.S.A.*

**ABSTRACT**

We describe a test of Local Position Invariance to be performed by comparing mechanical and atomic clocks in a null gravitational redshift experiment. This experiment will be placed in a 650 km polar orbit as a co-experiment of the Relativity Mission (also known as Gravity Probe B, GP-B). The mechanical clocks are provided by the rotation of the GP-B high precision orbiting gyroscopes, while the atomic clocks are Earth based and referenced to the satellite by GPS. The goal is to measure the gyroscope clock frequencies to an accuracy of 0.01% of the gravitational redshift due to the eccentricity of the orbit of the Earth about the Sun. This corresponds to an integrated frequency measurement over one year of $\Delta\nu/\nu = 3\times10^{-14}$. We present an analysis of the main torques which disturb the gyroscope clocks. The dominant torque is due to fluctuations in the molecular drag of the residual gas (caused by temperature variations), and is minimized by using a low temperature bake-out technique in order to achieve the required vacuum of $10^{-14}$ Pa. We compare results of ground based (flight prototypical) gyroscope clock experiments with the numerical simulations of the major disturbance torques. Effects due to cosmic radiation, precession, polhoding, and the readout system are also discussed.

## *I. INTRODUCTION*

The Gravity Probe B Relativity Mission (GP-B)[1] will measure in an 18 months space flight the frame dragging and geodetic rotational effects predicted by gravitational theories. $\dot{\Omega}$, the precession of a gyroscope in circular orbit, is given by metric gravitational theories in the PPN formalism[2] by:

$$\vec{\Omega} = \left(\gamma + \frac{1}{2}\right)\frac{GM}{c^2 R^3}\left(\vec{R} \times \vec{v}\right) + \left(\gamma + 1 + \frac{\alpha_1}{4}\right)\frac{GI}{2c^2 R^3}\left[\frac{3\vec{R}}{R^2}\cdot\left(\vec{\omega}_e \cdot \vec{R}\right) - \vec{\omega}_e\right] \qquad (1)$$

where $\dot{R}$ and $\dot{v}$ are the location and the orbital velocity of the gyroscope, and I, M, and $\dot{\omega}_e$ are the moment of inertia, the mass, and the angular velocity of the Earth.

In General Relativity $(\gamma = 1, \alpha_1 = 0)$ the geodetic precession, represented by the first term of Eq. 1, is 6.6 arcsec/yr in a 650 km polar orbit, and will be measured to about one part in $10^5$. Frame dragging, expressed by the second term of Eq. 1, is 0.033 arcsec/yr for a gyroscope with the spin axis pointed to the star HR5110 (37 degrees declination). This effect will be measured for the first time and with an accuracy of about three parts in $10^3$.

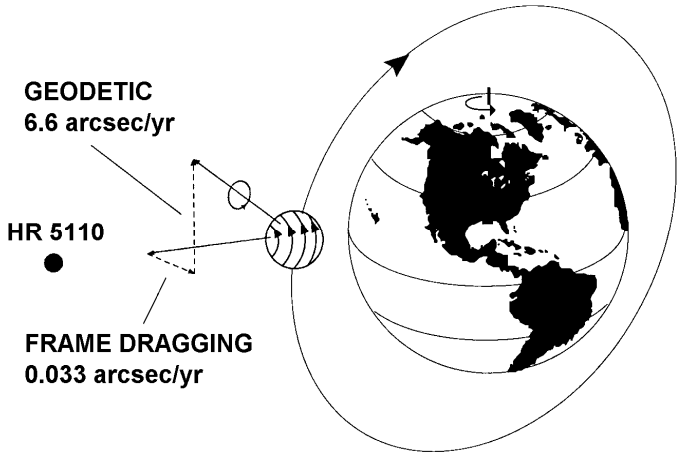


*Figure 1. GP-B experimental concept*

The precession $\dot{\Omega}$ is determined by measuring the variation of the angle between the local frame of reference, as determined by the gyroscopes, and the universal inertial frame, as determined by a telescope pointed to the star HR5110. The proper motion of this star has been measured independently to 0.1 marcsec/yr. Figure 1, shows schematically the precession due to the geodetic and frame dragging effects. In a polar orbit these two effects are orthogonal to each other.

In order to achieve the measurement accuracy, the total drift rate of the gyroscopes, without compensating with modelling, must be less than or equal to 0.1 marcsec/yr ($3\times10^{-12}$ deg/h). Note that the error budget for the experiment is distributed approximately equally between the gyroscope drift and the two main other error sources; the gyroscope readout noise and the proper motion of the guide star. The orbiting gyroscope is necessarily shielded to a very high degree from all disturbing torques, consequently allowing the opportunity of using it as a mechanical clock.[4] Section II is a discussion of the GP-B gyroscope implementation and of the features which allow its use as a very precise clock. Section III contains an overview of the main disturbance effects on the gyroscope clock.

## `II. THE GYROSCOPE CLOCK

The $3\times10^{-12}$ deg/h drift rate of the GP-B gyroscopes represents an improvement of more than ten orders of magnitude over the about $10^{-1}$ deg/h raw drift rate, (without modelling), exhibited by the best conventional ground based gyroscopes. The three main techniques which make this improvement possible are: the ultralow gravity environment, very high precission spherical geometry for the gyroscope rotors, and the averaging of the disturbing torques by rolling around the spin axis. Firstly, in order to reduce the torques caused by the suspension system the gyroscopes are placed in a satellite in which the residual drag is being compensated. The resulting acceleration is between $10^{-11}$ and $10^{-12}$ *g*, the Earth's gravitational acceleration. Secondly, the gyroscope rotors are made of fused quartz or single crystal silicon with a density variation over the 3.8 cm diameter $D$ of $\delta\rho/\rho \le 2\times10^{-7}$. Polishing and precision processing insure that the variation of the diameter is kept to $\delta D/D \le 10^{-6}$. Thirdly, the spacecraft will roll around the gyroscope spin axis, (which is also the line of sight to the guide star), with a period of 60-180 s. The alignment between the spacecraft roll axis and the gyroscope spin axis will be better than 10 arcsec, thus reducing the remaining precessional disturbance torques by a factor of about $5\times10^{-5}$.

Additional gyroscope drift is caused by thermal and cosmic radiation effects, residual gas drag, and electromagnetic disturbances. The gyroscope is operated at 2.5 K, and therefore thermal drift disturbances are minimized. In order to avoid problems of differential thermal expansion the gyroscope housing is also made of fused quartz. Figure 2 is an exploded schematic view of the gyroscope and the gyroscope housing.

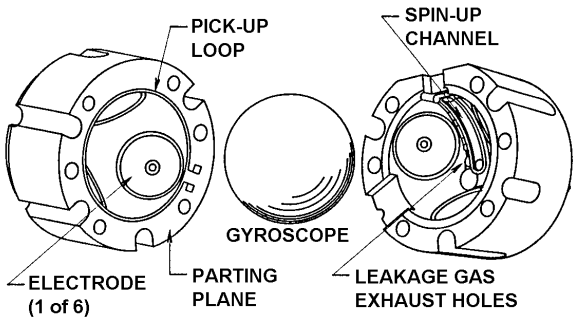


*Figure 2. Schematic view of gyroscope.*

Three pairs of orthogonal electrodes coated on the housing serve to suspend the rotor electrostatically, and to sense its position and charge. Minimization and optimization of the voltages applied to the electrodes and of the rotor charge are essential in order to achieve the required drift rate. Charging of the rotor by cosmic radiation is compensated for by a charge control system using ultraviolet photoemission.[5)]

The gyroscopes are spun to 100-120 Hz using 7 K helium gas. After the spin-up the required vacuum level of about $10^{-9}$ pa is achieved using a low temperature bakeout technique. Angular momentum readout is based on the measurement of the magnetic dipole moment (aligned with the spin axis) which is produced by a rotating superconductor.[6)] The magnetic dipole for the gyroscope is created by the 1.2 μm niobium coating of the spinning rotor. It is then detected by a superconducting loop

located on the parting plane of the gyroscope housing and coupled to a low noise dc SQUID magnetometer. Due to both readout and torque requirements, the dc magnetic field at the gyroscopes is kept at less than $2\times10^{-7}$ gauss, while the attenuation factor for ac magnetic fields is in excess of $10^{12}$.

To summarize, the main features (already incorporated in the GP-B experiment) that make the gyroscope a very precise clock useful for gravitational redshift measurements are as follows:

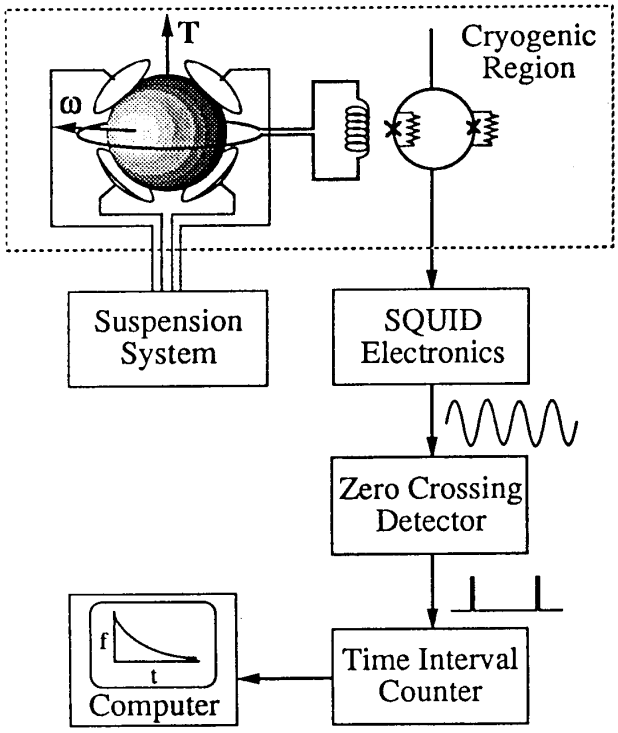


*Figure 3. Diagram of gyroscope clock.*

a) an environment with minimized torques.

b) a magnetic readout system measuring spin phase relative to the distant stars, which insures a frequency stability in the range:
$3\times10^{-14}\cdot\mathrm{yr}^{-1}\le\Delta\nu/\nu\le3\times10^{-12}\cdot\mathrm{yr}^{-1}$.

c) a GPS receiver which allows time transfer from Earth based atomic clocks.

d) a stable phase reference to the rolling spacecraft implemented by using a star blipper.

e) an experimental lifetime of 1.5 years, allowing closure and overlap in the data measuring the yearly variation of the gravitational field caused by the eccentricity of the Earth orbit around the Sun.

Figure 3 shows a conceptual diagram of the gyroscope clock, its instrumentation, and its data acquisition system.

### *III. MAIN DISTURBANCE EFFECTS*

One of the possible applications of a mechanical clock is a null gravitational redshift measurement. This experiment will compare the frequency of the orbiting gyroscope to that of Earth based atomic clocks. The eccentricity of the orbit of the Earth around the Sun causes an annual variation in the gravitational redshift of $\Delta\nu/\nu=3\times10^{-10}$. A null result would mean equal gravitational redshift for the atomic and gyroscope clocks, therefore verifying the equivalence principle. This experiment will extend gravitational redshift observations to clocks based on the spin speed of a rotating mass.

The measurement can also be interpreted as a check of the invariance of the fine structure constant $\alpha$. Atomic clock frequencies depend on $\alpha^4$, while the mechanical gyroscope frequency varies as $\alpha^2$. The best null-gravitational redshift experiment to date

gives a result consistent with zero to 2%, when comparing the redshifts of a hydrogen maser and a superconducting cavity stabilized oscillator.[7] We discuss the disturbance torques in terms of two levels of accuracy for a null gravitational redshift experiment. A minimal 1% measurement, $\Delta\nu/\nu = 3\times10^{-12}\cdot\mathrm{yr}^{-1}$, and a precise 0.01% experiment, $\Delta\nu/\nu = 3\times10^{-14}\cdot\mathrm{yr}^{-1}$. The frequency measurement for the lower accuracy can be performed by the existing GP-B electronic system, while the higher accuracy would require some improvements in the gyroscope frequency measurement system.

### *A. Molecular Drag and the Low Temperature Bake-out*

Molecular drag represents the major disturbance torque for the gyroscope clock. Note that while gyroscope housing symmetry and spacecraft roll reduced the precession torque by more than $5\times10^{-6}$, the residual gas spin-down torque is not similarly reduced. The gyroscope clock is therefore critically sensitive to both the residual gas pressure and its variation. Molecular drag causes exponential spin-down with a time constant $\tau$:

$$\tau = \frac{3}{10}\cdot\frac{M}{P\cdot r^2}\cdot\sqrt{\frac{k_B\cdot T}{2\cdot\pi\cdot m_{He}}} \tag{2}$$

where $M = 64\mathrm{g}$, $r = 1.9\mathrm{cm}$, and $T = 2.5\mathrm{K}$ are the mass radius and temperature of the gyroscope, $P$ and $m_{He}$ are the pressure and atomic mass of the helium gas, and $k_B$ is Boltzman's constant. For a time interval $\Delta t$ the resulting fractional frequency variation is:

$$\frac{\Delta\nu}{\nu} = \frac{\Delta\mathrm{t}}{\tau} \cong 10^{-3}\cdot\Delta\mathrm{t}\cdot\mathrm{P}\,(\mathrm{Pa}) \tag{3}$$

With no modelling, the pressure requirement for the high accuracy measurement is $\mathrm{P} \le 10^{-18}\,\mathrm{Pa}$, while the gyroscope precession measurement requires only $\mathrm{P} \le 10^{-9}\,\mathrm{Pa}$. In order to reduce the pressure, subsequent to the introduction of the helium gas used for spin-up, we utilize a low temperature bakeout technique. Similar to standard bakeout, the temperature of the surfaces is raised, thus promoting helium desorption, while simultaneously the desorbed gas is pumped out from the probe. In addition, exploiting the large binding energy of helium on metals, the remaining gas is adsorbed subsequent to the cool-down in a surface sub monolayer. The binding energy is typically $E_B/k_B \approx 150\mathrm{K}$.[8]

Pumping out a volume $V$ to the pressure $P_1$ at the bake-out temperature $T_1$, will result (in the ideal case) in the pressure $P_2$ at temperature $T_2$ being:

$$\frac{\boldsymbol{P_2}}{\boldsymbol{P_1}} = \left(\frac{\boldsymbol{T_2}}{\boldsymbol{T_1}}\right)^{3/2}\cdot\exp\left[\frac{\boldsymbol{E_B}}{\boldsymbol{k_B}}\cdot\left(\frac{\boldsymbol{1}}{\boldsymbol{T_1}}-\frac{\boldsymbol{1}}{\boldsymbol{T_2}}\right)\right] \tag{4}$$

Equation 4 is valid for the case of small volume to area ratio $V/A$:

$$\boldsymbol{V/A} << \boldsymbol{\lambda}\cdot\exp\left(\boldsymbol{E_B/k_BT}\right)\ \text{where}\ \boldsymbol{\lambda} \equiv \left(\boldsymbol{h^2/2\pi\cdot m_{He}k_BT}\right)^{1/2} \tag{5}$$

where $\lambda$ is the de Broglie thermal wavelength, all helium atoms are assumed to reside on the surface at $T_2$, and the surface density $\sigma$ is related to the volume density $n$ by:

$$\boldsymbol{\sigma = n\lambda \cdot \exp\left(E_B / k_B T\right)} \tag{6}$$

For the GP-B operational conditions, $\boldsymbol{T_1 = 7.5\text{K}, T_2 = 2.5\text{K}, \left(P_1 \le 10^{-5}\ \text{Pa}\right)}$, the expected pressure reduction factor is: $P_2/P_1 \le 5\times10^{-17}$. In practice this factor is not fully achievable due to the open cell geometry, the gas desorption from the higher temperature regions, and the non-complete bakeout of all surfaces. In practice, using the low temperature bakeout and an additional large area adsorption pump, we expect to achieve a gyroscope pressure at 2.5 K of $10^{-13}$ -$10^{-15}$ Pa. This requires that the spin-down due to residual gas should be modelled to $10^{-1}$-$10^{-3}$ and to $10^{-3}$-$10^{-5}$, for the $10^{-2}$ and the $10^{-4}$ versions of the null gravitational experiment respectively.

***B. TEMPERATURE FLUCTUATIONS***

Temperature fluctuations of the gyroscope clock are caused by variations in the thermal control of the support structure and by the heating produced by cosmic radiation. The two mechanisms by which temperature fluctuations cause clock frequency variations are: a) residual pressure variations caused by gas desorption from the gyroscope housing, and b) changes in the moment of inertia of the rotor due to thermal expansion. Note that helium desorption from the rotor does not change the frequency, because to first order the pressure is determined by the gyroscope housing and support structure, which are colder and have larger surfaces than the rotor.

The fractional pressure variation $\Delta P/P$ caused by a temperature variation $\Delta T$ is:

$$\boldsymbol{\frac{\Delta P}{P} = \frac{\Delta T}{T}\left(\frac{3}{2} + \frac{E_B}{k_B T}\right) \cong 60\frac{\Delta T}{T}} \tag{7}$$

Assuming a linear temperature drift $\Delta T/\Delta t$ of the gyroscope housing, the resulting yearly fractional frequency variation from Eqs. 3 and 7 will be:

$$\boldsymbol{\frac{\Delta \nu}{\nu} \cong 4\times10^{5} \cdot P\left(\text{Pa}\right) \cdot \frac{\Delta T}{\Delta t}\left(\text{K}\cdot\text{yr}^{-1}\right)} \tag{8}$$

$$\frac{\Delta\nu}{\nu} = 3\times10^{-12}\ \text{yr}^{-1} \Rightarrow \text{P}\frac{\Delta\text{T}}{\Delta\text{t}} \le 10^{-17}\ \text{Pa}\cdot\text{K} \Rightarrow \text{P} = 10^{-13}\ \text{Pa},\ \frac{\Delta\text{T}}{\Delta\text{t}} = 10^{-4}\ \text{K}\cdot\text{yr}^{-1} \tag{8a}$$

$$\frac{\Delta\nu}{\nu} = 3\times10^{-14}\ \text{yr}^{-1} \Rightarrow \text{P}\frac{\Delta\text{T}}{\Delta\text{t}} \le 10^{-19}\ \text{Pa}\cdot\text{K} \Rightarrow \text{P} = 10^{-14}\ \text{Pa},\ \frac{\Delta\text{T}}{\Delta\text{t}} = 10^{-5}\ \text{K}\cdot\text{yr}^{-1} \tag{8b}$$

Equations 8a and 8b show the pressure and temperature stability requirements needed for the low and high accuracy clock measurements. These requirements are well within the capabilities of the GP-B experiment.

Large temperature fluctuations, causing significant changes in the moment of inertia of the rotor, are caused by cosmic radiation and by the initial heating during the low

temperature bakeout process. The temperature increase $\Delta T$, the frequency variation $\Delta\nu/\nu$, and the time constant for thermal relaxation by black body radiation $\tau_B$ are:

$$\Delta T = \frac{E_T}{C_0 T^3} \qquad \frac{\Delta\nu}{\nu} = 2\cdot\alpha\cdot\Delta T = \frac{2\cdot\alpha\cdot E_T}{C_0 T^3} \qquad \tau_B \cong \frac{C_0}{4\cdot\varepsilon\cdot\sigma\cdot A} \tag{9}$$

where $C_0 T^3$, $\alpha$, $\varepsilon \approx 0.05$, and $A$=45×10$^{-4}$m$^2$, are the heat capacity, linear expansion coefficient (at about 3 K), thermal emissivity, and area of the rotor. $E_T$ is the total heat input (over a time short compared to $\tau_B$) and $\sigma$ is the Stefan-Boltzman radiation constant. Table I gives the thermal parameters for fused quartz and silicon rotors assuming heating by a major solar flare which deposits $E_T = 10^{-3}$ J in the rotor.

Table I. Thermal parameters for 1 mJ energy deposition in quartz and silicon rotors.

| **Rotor** | **C0** (J·K$^{-4}$) | $\alpha$ (K$^{-1}$) | $\Delta T$ (K) | $\Delta\nu/\nu$ | $\tau$ (days) |
|---|---|---|---|---|---|
| **Fused Quartz** | 2.6×10$^{-4}$ | -7×10$^{-9}$ | 0.14 | -2×10$^{-9}$ | 50 |
| **Single Crystal Silicon** | 1.7×10$^{-5}$ | 7×10$^{-12}$ | 2.18 | 3×10$^{-11}$ | 4 |

From table I we conclude that single crystal silicon rotors are preferable for clock applications, as their frequency variations are smaller by two orders of magnitude and their radiative time constant shorter by one order of magnitude compared with fused quartz rotors. The disadvantage of the larger temperature increase for silicon is mitigated by the much shorter radiative time constant. Using information provided by cosmic radiation detectors, the major frequency excursions can be easily removed from the data, while moderate frequency variations can be modeled to achieve $\Delta\nu/\nu = 3\times10^{-14}$ yr$^{-1}$.

### *C. OTHER DISTURBANCE TORQUES*

Table II summarizes the main disturbance torques and their effects on the frequency stability of the gyroscope clock. The first three torques have been discussed in the previous sections, with the remaining major effects caused by rotor charging, imperfections in rotor geometry, and the readout system. Only effects resulting in yearly fractional frequency variations of the order of 10$^{-14}$ are considered.

Rotor charging causes frequency independent spin-down, with a rate *df/dt* measured to depend on the rotor potential $V_R$ as:

$$df/dt \cong 10^{-11}\cdot V_R^2 \ \text{Hz}\cdot\text{V}^{-2}\cdot s^{-1} \tag{10}$$

In order to achieve 3×10$^{-14}$ yr$^{-1}$ frequency stability the rotor potential will be measured to about 0.1 mV, and the data used to model and eliminate the spin-down disturbance. The readout system interacts with the dipole moment of the rotor producing a spin-down torque which is however less than 10$^{-14}$ yr$^{-1}$.

Table II. Main disturbance torques and their effects on the gyroscope clock.

| **TORQUE** | **EFFECT** | $\Delta\nu/\nu$ ($yr^{-1}$) | **Supplementary Requirements** |
|---|---|---|---|
| Residual Gas | Exponential spin-down | $<3\times10^{-14}$ | $P<10^{-14}$ Pa, data model |
| Temp. Fluctuations | Spin speed fluctuations | $<3\times10^{-14}$ | $\Delta T/\Delta t \le 10^{-5}$ K·$yr^{-1}$ |
| Cosmic Radiation | Spin speed fluctuations | $<3\times10^{-14}$ | Data model |
| Rotor Charge | Spin-down | $<3\times10^{-14}$ | Charge measure |
| Readout System | Exponential spin-down | $<10^{-14}$ | |
| Mass Unbalance and Rotor Asphericity | Spin speed modulated at polhode frequency | $<10^{-14}$ | Analog filter and data model |

The mass unbalance and rotor asphericity torques can be significantly reduced by using the gyroscope in the drag free sensor position as the primary clock. As the rotor of the drag free sensor is not levitated, (spacecraft control keep it centered in the housing), no electrostatic torques act on it. In addition filtering of the spin speed frequency in the position sensing system and data modeling are required to meet the $10^{-14}$ frequency stability performance.

## *IV. CONCLUSIONS*

The drag free sensor gyroscope of the GP-B Relativity Mission can be used directly as a mechanical clock with frequency stability of $\Delta\nu/\nu = 3\times10^{-12}$ $yr^{-1}$, provided that the rotor is made of single crystal silicon. Achievable improvements in the areas of data modeling, probe vacuum, gyroscope temperature control, and rotor charge measurement will allow the frequency stability to reach $\Delta\nu/\nu = 3\times10^{-14}$ $yr^{-1}$.

## *ACKNOWLEDGMENTS*

This work was supported by NASA contract No. NAS8-39225.

## *REFERENCES*

**1)** J.P. Turneaure *et al*., Adv. Space Res. **9**, 29 (1989)
**2)** C.M. Will, *Theory and Experiment in Gravitational Physics* (Cambridge University Press, Cambridge, England, 1993)
**3)** C.W.F. Everitt and Saps Buchman, *Particle Astrophysics, Atomic Physics and Gravitation* pp 467 (Editions Frontieres, Cedex, France, 1994)
**4)** Todd Walter, *Ph.D. Thesis*, (Stanford University, Stanford, USA, 1993)
**5)** Saps Buchman *et al*., Rev. Sci. Instrum. **66**, 120 (1995)
**6)** F. London, *Superfluids* (Dover, New York, 1961)
**7)** J.P Turneaure *et al*., Phys. Rev. D **27**, 1705 (1983)
**8)** J.P Turneaure *et al*., *Near Zero,* (W.H.Freeman and Co., New York, 1988) pp 671